Rapid measurement of surface acoustic wave velocity on single crystals using an all-optical adaptive scanning acoustic microscope

Y. Hong, S. D. Sharples, M. Clark, and M. G. Somekh[a]
School of Electrical and Electronic Engineering, University of Nottingham, United Kingdom, NG7 2RD

(Received 5 May 2003; accepted 29 August 2003)

An experimental method has been developed to measure the phase velocity of laser-generated and detected surface acoustic waves. An optical grating produced by a spatial light modulator was imaged onto the sample surface to generate the ultrasound whose frequency and wave front were controlled electrically by tailoring the grating. When the grating period matched the surface acoustic wavelength, strong excition of the surface wave was observed. Thus, the wavelength and, thereby, the phase velocity were determined. We present results with this method that allow the phase velocity and the angular dispersion of the generalized surface wave as well as the pseudosurface wave on the (100) nickel and (111) silicon single crystals to be measured, with the precision of approximately 0.2%. Those factors affecting the measurement precision are discussed. © *2003 American Institute of Physics.* [DOI: 10.1063/1.1621091]

Surface acoustic waves (SAWs) have been extensively studied to characterize the elastic properties of materials. The phase velocity is of particular importance because it is directly related to the wave equation, allowing extraction of the elastic constants and, in the case of single crystals, the crystallographic orientation. Many techniques have been developed to determine the phase velocity of SAWs experimentally, including ultrasonic reflectivity,[1] acoustic microscopy,[2] and more recently Brillouin scattering.[3–5] Among these techniques, such contact techniques as ultrasonic reflectivity and acoustic microscopy either suffer from the couplant perturbation or are restricted by the transducer dimension. Although, Brillouin scattering is noncontact, a high-quality sample surface is required and the signal-to-noise ratio (SNR) tends to be rather poor due to the small proportion of Brillouin scattered photons resulting in extremely long measurement time. It has also been reported that there is a 3%–4% systematic error in this measurement.[3–5] In the last two decades, the laser generation and detection of ultrasound has been developed and proved to be a powerful tool to investigate SAWs. As a noncontact technique, it can work in hazardous environments and provide reliable measurements. By exploring the transient SAW pulse generated by a short laser pulse, the phase velocity can be determined accurately.[6,7] But, to obtain high temporal resolution, high-energy laser pulses are required, which can cause damage to the sample. Moreover, the detection sensitivity is relatively low because the generated SAWs are broadband signals. To improve detection sensitivity without causing damage, some narrow-band schemes have been proposed that used line arrays instead of a single line as the generating source.[8,9] As a result of narrowing signal bandwidth, the SNR can be improved. However, it is difficult for those narrow-band schemes to produce line arrays with uniform spacing and intensity, which thus degrades the SNR improvement as expected.[9] The other difficulty, in practice, is to control the optical distribution of line arrays.

To overcome such difficulties, the authors have constructed an all-optical adaptive scanning acoustic microscope (O-SAM) with a spatial light modulator (SLM) to control the source distribution.[10] The use of the SLM allows us to generate arbitrary optical distributions from the source laser. The benefits are twofold: (1) By spreading the energy of the source laser, large SAW amplitudes can be generated below the damage threshold, and (2) by tailoring the optical distribution of the source laser, the frequency and wave front of the SAWs can be controlled in real time, which enables it to adapt to variations in material properties. In this letter, we report a method using the O-SAM to measure the phase velocity of surface waves. Experimental results on single crystals are presented and the factors affecting the measurement precision and accuracy are discussed.

A schematic diagram of the O-SAM is shown in Fig. 1. Its detailed construction has been described elsewhere.[11,12] Briefly, a Q-switched mode-locked Nd–YAG laser (1064 nm radiation wavelength, 82 MHz fundamental frequency) was used as the generating source. This optical energy from the pulsed laser was imaged to a size of 2.4 mm on the sample surface using the SLM; the image contained 512×512 programmable pixels. By programming the image on the SLM, the optical distribution of the source could be tailored,

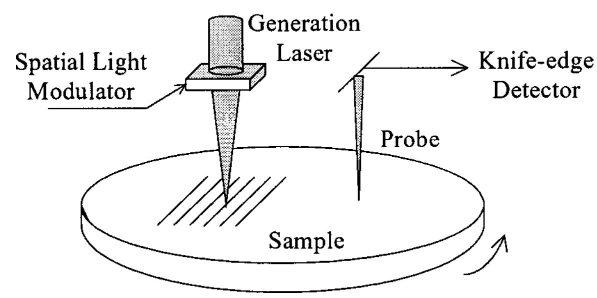

FIG. 1. Schematic diagram of experiment.

[a]Electronic mail: mike.somekh@nottingham.ac.uk

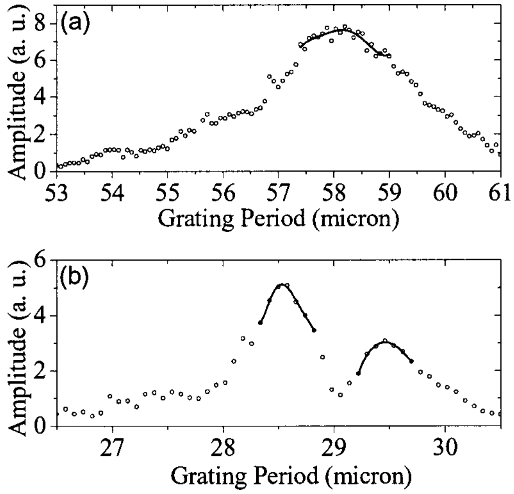

FIG. 2. Signal amplitude (circle) with grating period when propagating along 22° on the (111) oriented silicon, (a) at 82 MHz, (b) at 164 MHz, along with the fitting curve (solid).

thereby controlling the properties of generated ultrasound. The ultrasound was detected with an optical knife-edge detector. To perform velocity measurement, the source pattern was set as a grating with the lines spaced uniformly to generate SAWs with a planar wave front. The detector was positioned approximately 2 mm from the center of the source. The output of the detector was observed and recorded with an oscilloscope. In the experiment, the grating period was changed progressively by programming the image parameters on the SLM. When the period matched the SAW wavelength, either at the fundamental frequency or a harmonic thereof, a maximal excitation in the strength of the SAWs was observed. The resulting signal was then Fourier transformed to get the signal strength at the generation frequency so that a plot of signal strength as a function of grating period was obtained, as shown in Fig. 2. Experimental values around the peak were smoothed with the polynomial. The peak of the smoothed curve corresponds to the wavelength of generated ultrasound, allowing the phase velocity to be determined. The whole experiment was controlled by software and there was no mechanical movement involved, thus any uncertainty introduced by distance or time measurement was avoided.

The generation mechanism of the method is general so that it can work on both metals and dielectrics.[11] In this letter, experiments were performed on a block of (100) oriented single crystal nickel, and an (111) oriented single crystal silicon wafer. The silicon wafer was 300 μm thick. As it is transparent at the radiation wavelength (1064 nm), a 30 nm chrome thin film was coated on the surface to generate the acoustic wave efficiently, which would be unnecessary if a different wavelength was used. The angular dispersions of the samples were obtained by rotating the sample to measure the phase velocities along different propagation directions. The theoretical velocity was calculated with the partial wave method developed by Farnell *et al.*[13] and used the elastic constants in Ref. 14.

On the (001) plane of Ni, the measured phase velocities agreed well with theoretical values to within 10 ms^{-1} (Fig. 3), both for the generalized SAW (GSAW) and for the pseudosurface acoustic wave (PSAW). The phase velocities of the slow transverse wave (STW) are also displayed. The angular dispersion of experimental velocities shows mirror symmetry about 45° as expected. We noted that, in the directions between 32° and 60°, the experimental velocity shows a sharp increase to the PSAW branch and the GSAW signal disappears. In these directions, calculation reveals that the penetration depth of GSAW increases gradually and it behaves more like a bulk wave. As 45° approaches, it degenerates into a STW that is polarized transversely to its propagation direction. This tendency is accompanied with a decrease of normal displacement. Since the knife-edge detection relies on the gradient of the surface displacement, the GSAW signal will vanish when it decreases beyond the detector sensitivity. Meanwhile, the PSAW, a high-speed SAW mode which radiates energy into the bulk and attenuates while propagating, emerges at 32° and diminishes at 58°. The attenuation on the (100) oriented Ni, however, is so small that the wave is easily detected in the experiment.

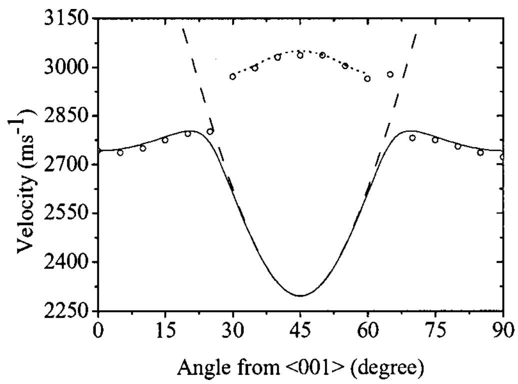

FIG. 3. Angular dispersions of the measured phase velocities (circle) at 82 MHz and the theoretical velocities of GSAW (solid), PSAW (dotted), and STW (dashed) on the (100) oriented nickel.

Figure 4 shows the phase velocities measured between the ⟨110⟩ and ⟨100⟩ directions on the (111) oriented silicon, along with the theoretical velocities of GSAW and STW. As expected, the angular dispersion of experimental velocities had mirror symmetry about the direction of 30° and hexagonal symmetry in general. Notably, besides the GSAW, another wave mode was observed in all directions, which reproduced the symmetry of the GSAW but propagated with a higher velocity. The velocities of this wave approached those of the STW in some directions and were lower than the the-

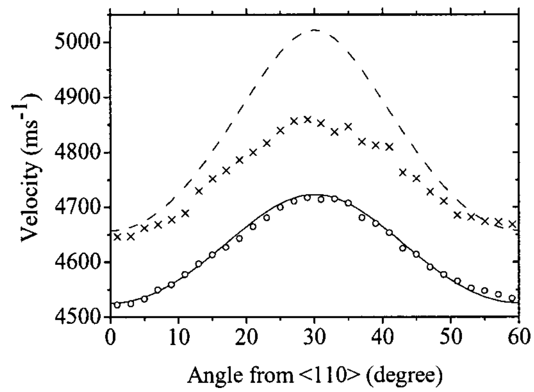

FIG. 4. Angular dispersions of the measured phase velocities of SAW (circle), the faster wave (cross) at 164 MHz and the theoretical velocities of GSAW (solid), STW (dashed) on the (111) oriented silicon.

oretical velocities of the PSAW (5300–5700 ms^{-1}). Considering the case of the Lamb wave in isotropic substrate, as the substrate thickness increases, the velocities of the a_0 and s_0 Lamb modes converge to the GSAW velocity and the velocities of the higher Lamb modes approached that of the STW.[15] The thickness of the silicon wafer used here was about 300 μm, far greater than the Lamb wavelengths. In this case, the faster wave observed is likely to be some higher-order Lamb mode. Further experimental work, including dispersion and attenuation measurements, is still needed to identify this mode. It is also noteworthy that this wave was only observable when excited at harmonic frequencies of 164 MHz or more. The signal amplitude as a function of grating period at the direction of 22° is shown in Fig. 2. The first peak in Fig. 2(b) corresponds to the GSAW and the second corresponds to the faster wave. When excited at 82 MHz [Fig. 2(a)], the two peaks overlapped with each other and the maximum occurred in the middle of them. They were not so well resolved at 82 MHz because there were fewer grating periods so the relative wavelength resolution was poorer. Thus, by the higher-frequency excitation, it is possible to distinguish the multiple wave modes as this can provide better resolution.

In this letter, we have achieved measurement precision of approximately 0.2%, the method is at an early stage of development, but it is worth discussing some of the factors that may limit both the precision and the accuracy of the method. (1) The velocity is measured under the laser radiation. The slight dc heating caused by laser could depress the velocity slightly. (2) The limit of spatial resolution of the grating period is approximately 0.8 μm, which means that the precise SAW wavelength cannot be projected onto the sample, however, the excitation strength is a smooth function of grating period around the peak. Fitting a polynomial around this peak and taking the maximum of the polynomial ensures that the precision of determining the peak position is limited by SNR rather than quantization errors. (3) The uncertainty in the precise value of grating period due to the optical defocus errors might account for the main systematic errors in this method. These defocus errors can be eliminated by calibrating the size of the SLM image.

The method as presented offers a rapid, convenient, noncontact, and precise method of the phase velocity determination without recourse to the mechanical movement. A modification to the method involving scanning the probe outside the excitation region could offer extreme measurement precision by determination of the phase gradient.

[1] F. R. Rollins, T. C. Lim, and G. W. Farnell, Appl. Phys. Lett. **12**, 236 (1968).
[2] W. Parmon and H. L. Bertoni, Electron. Lett. **15**, 684 (1979).
[3] M. Mendik, S. Sathish, A. Kulik, G. Gremaud, and P. Wachter, J. Appl. Phys. **71**, 2830 (1992).
[4] P. R. Stoddart, J. D. Comins, and A. G. Every, Phys. Rev. B **51**, 17574 (1995).
[5] M. H. Kuok, S. C. Ng, Z. L. Rang, and T. Liu, Solid State Commun. **110**, 185 (1999).
[6] A. Neubrand and P. Hess, J. Appl. Phys. **71**, 227 (1992).
[7] H. Coufal, K. Meyer, R. K. Grygier, P. Hess, and A. Neubrand, J. Acoust. Soc. Am. **95**, 1158 (1994).
[8] J. Jarzynski and Y. H. Berthelot, J. Acoust. Soc. Am. **85**, 158 (1989).
[9] J. Huang, S. Krishnaswamy, and J. D. Achenbach, J. Acoust. Soc. Am. **92**, 2527 (1992).
[10] S. D. Sharples, M. Clark, and M. G. Somekh, Appl. Phys. Lett. **81**, 2288 (2002).
[11] M. Clark, S. D. Sharples, and M. G. Somekh, IEEE Trans. Ultrason. Ferroelectr. Freq. Control **47**, 65 (2000).
[12] M. Clark, S. D. Sharples, and M. G. Somekh, Meas. Sci. Technol. **11**, 1792 (2000).
[13] G. W. Farnell, *Properties of Elastic Surface Waves*, Physical Acoustics Vol. 6, edited by W. P. Mason and R. N. Thurston (Academic, New York, 1970), pp. 109–166.
[14] B. A. Auld, *Acoustic Fields and Waves in Solids* (Wiley, New York, 1973), Vol. 1, Appendix 2.
[15] I. A. Viktorov, *Rayleigh and Lamb Waves* (Plenum, New York, 1967), Chap. 2.